ZSPA presents no problems for the solution of the ME equation. The influence on the ME density map of the introduction of the ZSPA is insignificant.

References

BRICOGNE, G. & GILMORE, C. J. (1990). *Acta Cryst.* A**46**, 284–297.
COLLINS, D. M. (1982). *Nature (London)*, **298**, 49–51.
GILMORE, C. J., BRICOGNE, G. & BANNISTER, C. (1990). *Acta Cryst.* A**46**, 297–308.
GULL, S. F. & DANIEL, G. J. (1978). *Nature (London)*, **272**, 686–690.
SAKATA, M., MORI, R., KUMAZAWA, S., TAKATA, M. & TORAYA, H. (1990). *J. Appl. Cryst.* **23**, 526–534.
SAKATA, M. & SATO, M. (1990). *Acta Cryst.* A**46**, 263–270.
SAKATA, M., UNO, T., TAKATA, M. & HOWARD, C. J. (1993). *J. Appl. Cryst.* **26**, 159–165.
SAKATA, M., UNO, T., TAKATA, M. & MORI, R. (1992). *Acta Cryst.* B**48**, 591–598.
WILKINS, S. W., VARGHESE, J. N. & LEHMANN, M. S. (1983). *Acta Cryst.* A**39**, 47–60.

Acta Cryst. (1995). A**51**, 53–60

A New Commensurate Modulated Structure in Orthoclase

BY HUIFANG XU*

Department of Earth and Planetary Sciences, The Johns Hopkins University, Baltimore, Maryland 21218, *USA, and Department of Earth Sciences, Nanjing University, Nanjing, Jiangsu* 210008, *People's Republic of China*

DAVID R. VEBLEN

Department of Earth and Planetary Sciences, The Johns Hopkins University, Baltimore, Maryland 21218, *USA*

AND GUFENG LUO

Department of Earth Sciences, Nanjing University, Nanjing, Jiangsu 210008, *People's Republic of China*

(*Received* 2 *April* 1994; *accepted* 9 *June* 1994)

Abstract

Transmission electron microscopy shows that there is an ordered modulated structure in orthoclase ($Or_{84.6}Ab_{13.1}An_{2.3}$) (Or = orthoclase, Ab = albite, An = anorthite) of an augite monzonite from Wulian, Shandong Province, Northern China. The modulated orthoclase is composed of a series of triclinic (010) layer domains with $C\bar{1}$ symmetry. Each domain has a thickness of $4d_{010}$ and the domains are periodically arranged along the b axis. The modulation period along the b axis is thus 104 Å ($=8d_{010}$). The relationship between the extended unit-cell parameters of the modulated structure (supercell) and the triclinic subcell parameters is: $a_{sup} \simeq a_{sub}$; $b_{sup} = 8d_{010} \simeq 8b_{sub}$; $c_{sup} \simeq c_{sub}$; $\beta_{sup} \simeq \beta_{sub}$. The probable space group of the commensurately modulated orthoclase is Pm. The modulated structure probably forms during the phase transition from sanidine ($C2/m$ symmetry) to microcline ($C\bar{1}$ symmetry) through the segregation of Al atoms from T_2 sites into $T_{1(0)}$ and $T_{1(m)}$ sites, respectively, in neighboring domains, which are in the albite-twin relationship. The ordering of Al atoms in the tetrahedral sites during the phase transition results in a sinusoidal deviation of the crystal structure from monoclinic symmetry. The Al–Si distribution near the domain boundary positions is likely to be relatively disordered.

1. Introduction

In structure, orthoclase [$(K,Na)AlSi_3O_8$] can be considered to be a heterogeneous crystal composed of domains with triclinic symmetry. The twins are so fine in scale that experiments using light or X-rays indicate only an average monoclinic ($C2/m$) average structure, rather than the local triclinic ($C\bar{1}$) symmetry of the individual domains (Smith, 1974; Laves, 1950; Goldsmith & Laves, 1954). Orthoclase is generally considered to be a metastable phase between sanidine and microcline and represents a stage in the ordering of aluminium in the tetrahedral sites of potassium feldspar (Smith, 1974; Laves, 1950; Goldsmith & Laves, 1954; Ribbe, 1983). The ordering of aluminium and silicon in the tetrahedron sites, exsolution microstructures and tweed textures in alkali feldspars have been thoroughly studied both theoretically and experimentally (Ribbe, 1983;

* Author for correspondence. Present address: Department of Geology, Arizona State University, Tempe, Arizona 85287, USA.

McConnell, 1965, 1971; Yund, 1983; Nissen, 1967; McLaren, 1984; Eggleton & Buseck, 1980; Parsons, 1984; McLaren & Fitz Gerald, 1988). However, well ordered modulated structures induced by Al–Si ordering at the sanidine–microcline phase transition have not been reported.

A phase diagram for alkali feldspars (Smith & Brown, 1988) shows stability fields for sanidine ($C2/m$) and microcline ($C\bar{1}$), with a phase boundary between them at about 773 K for potassium-rich compositions (Fig. 1). There is no stability field for orthoclase or modulated alkali feldspars in the phase diagram. If potassium feldspar crystallizes at a temperature above the phase transition, it will have a homogeneous monoclinic structure and relatively disordered Al–Si distribution in the tetrahedral sites (Fig. 2*b*). As the temperature decreases through the phase-transition temperature, monoclinic potassium feldspar will transform into the triclinic structure, owing to ordering of aluminium from the $T_{2(0)}$ and $T_{2(m)}$ sites into the $T_{1(0)}$ or $T_{1(m)}$ site. (Here, we use a fixed reference frame for the site nomenclature that remains constant through the phase transition, rather than the usual convention of assigning $T_{1(0)}$ and $T_{1(m)}$ designations based on aluminium occupancy of the already ordered triclinic feldspar.) If aluminium preferentially occupies the $T_{1(0)}$ sites, the structure will distort into the triclinic-orientation variant illustrated in Fig. 2(*a*). Alternatively, if aluminium preferentially occupies the $T_{1(m)}$ sites, distortion will be to the triclinic orientation shown in Fig. 2(*c*). The orientations of Figs. 2(*a*) and (*c*) are in the albite-twin relationship. Since the probabilities for the two twin orientations forming at the phase transition from sanidine to microcline are identical in the absence of external strain, some sort of twin-domain texture with equal amounts of each orientation can be expected to form.

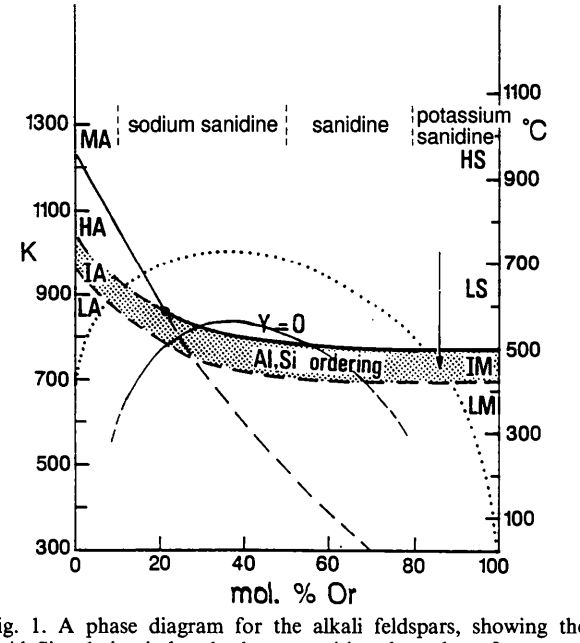

Fig. 1. A phase diagram for the alkali feldspars, showing the Al–Si-ordering-induced phase-transition boundary for potassium-rich alkali feldspars and the displacive phase-transition boundary for sodium-rich alkali feldspars. The equilibrium solvus (dotted) and coherent spinodal (solid and dashed) are also shown. (From Smith & Brown, 1988.) HS = high sanidine; LS = low sanidine; IM = intermediate microcline; LM = low microcline; MA = monalbite; HA = high albite; IA = intermediate albite; LA = low albite. The cooling path of the Wulian crystal is indicated by an arrow. Al–Si-ordering-induced phase transition of the orthoclase takes place before the solvus temperature is reached.

The geometrical arrangement of transformed triclinic cells gives rise to a range of diffraction phenomena in selected-area electron diffraction (SAED) patterns or other single-crystal diffraction patterns (McLaren & MacKenzie, 1976; Ribbe, 1983), as is illustrated schematically in Fig. 3. For homogeneous monoclinic or triclinic potassium feldspar (*i.e.* only one domain in a single orientation), the diffraction pattern shows only sharp Bragg reflections (Fig. 3*a*). For triclinic potassium feldspar composed of relatively large albite-twin domains arranged nonperiodically along the *b* axis, the diffraction pattern will show two sets of diffraction spots (like two diffraction patterns superimposed); there may also be diffuse streaking along the domain-stacking direction, depending on the domain size and shape and the radiation used (Fig. 3*b*). For triclinic potassium feldspar composed of fine layer-like albite-twin domains arranged periodically along the *b* axis, the SAED pattern depends upon the modulation period and radiation used (McLaren & MacKenzie, 1976). If the modulation period is about the same as or shorter than a coherent distance that was proposed by McLaren & MacKenzie (1976), the SAED pattern shows main Bragg reflections and discrete satellite reflections (Fig. 3*c*). However, if such planar fine-scale triclinic domains have variable thickness and are thus arranged nonperiodically, the diffraction pattern will show strong Bragg reflections and streaking along the domain stacking direction, but no satellite reflections (Fig. 3*d*). As pointed out by Ribbe (1983), it is theoretically possible to form a modulated structure in potassium feldspars during the Al–Si-ordering phase transition from sanidine ($C2/m$) to microcline ($C\bar{1}$) if the triclinic domains are arranged periodically in the albite-twin relationship, as shown schematically in Fig. 3(*c*). In this paper, we describe the natural occurrence of just such a one-dimensional commensurate modulated structure.

2. Sample and experimental methods

The orthoclase used in this study is from an augite monzonite from Wulian, Shandong Province,

Northern China. Its crystal shape is subhedral with a crystal size of 1–6 mm. The average composition determined by electron microprobe analysis is $Or_{84.6}Ab_{13.1}An_{2.3}$ (Pan, 1986). It displays monoclinic symmetry with the petrographic microscope, with optic angle ($-2V$) of 54 to 66° (Pan, 1986). X-ray powder diffraction also indicates a monoclinic structure. The monoclinic unit-cell parameters of the average structure are $a = 8.568$, $b = 12.980$, $c = 7.191$ Å and $\beta = 116.01°$. The sample corresponds to intermediate orthoclase, according to the classifications of Marfunin (1966), Wright & Stewart (1968) and Su, Bloss, Ribbe & Stewart (1984) for alkali feldspars.

For transmission electron microscopy (TEM) investigation, petrographic thin sections were prepared with a single polished surface and several suitable crystals were selected with the petrographic microscope and were mounted on Cu grids. The specimens for TEM were thinned with an argon ion mill and then coated with a thin carbon film. Electron microscopy study was performed with JEOL 200CX and Philips EM420ST transmission electron microscopes operated at 200 and 120 keV, respectively. High-resolution transmission electron microscopy (HRTEM) images were also obtained, with a JEOL 4000EX high-resolution electron microscope operated at 400 keV.

3. TEM and electron diffraction results

A [100] zone-axis SAED pattern (Fig. 4*a*) of this apparently monoclinic orthoclase sample shows up to four orders of satellite reflections flanking the main $0kl$ feldspar reflections and aligned along the b^* direction. The angle between **c*** and **b*** (*i.e.* α^*) is 90°. The modulation period indicated by the satellite reflections is $8d_{010} \simeq 8b$ of the substructure. The intensity of the satellite reflections decreases sharply with increasing order. Bright-field (BF) images formed by selecting the central beam and its nearby satellite reflections clearly show a one-dimensional modulation along the b axis (Fig. 4*b*) and the measured modulation period is about 104 Å ($=8d_{010}$). The (010) orientation of the modulation is consistent with the possibility that it is formed by periodic albite twinning of a triclinic substructure.

A [10$\bar{1}$] zone-axis SAED pattern also indicates the same modulation, as do the corresponding BF and dark-field (DF) images, formed from one main dif-

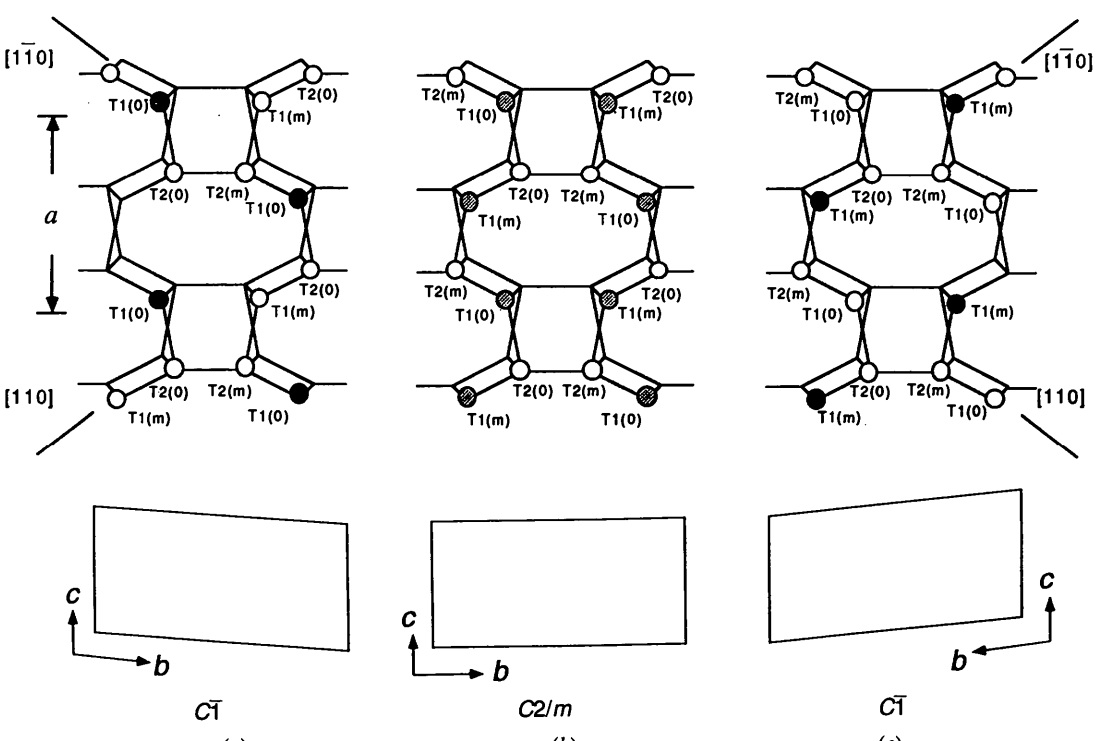

Fig. 2. (*a*) Triclinic distortion of the potassium feldspar structure due to aluminium ordering into the $T_{1(0)}$ site. (*b*) Relatively disordered distribution of Al and Si atoms in the sanidine structure and its monoclinic unit cell. (*c*) Triclinic distortion of the potassium feldspar structure due to aluminium ordering into the $T_{1(m)}$ site. Note that the site designations in the two triclinic orientations are in the fixed reference frame shown for the monoclinic structure in (*b*). Unfilled circles represent silicon-dominant sites; fully filled circles represent aluminium-dominant sites.

fraction spot and its nearby satellites (Fig. 5). The orthogonality of the [10$\bar{1}$] SAED pattern is consistent with overall monoclinic symmetry for the modulated structure. The crystal is dominated by a one-dimensional modulated structure along the *b* axis, which is very similar to a one-dimensional modulated orthoclase cited by Ribbe (1983, p. 25). No exsolution lamellae nearly parallel to (60$\bar{1}$) was observed in the crystal. In part of Fig. 5(*b*), there is a weak second modulation overlapping and normal to the main (010) modulation. This area of two-dimensional modulation is consistent with triclinic domains related by both the albite and pericline twin laws, analogous to the microstructures observed in tweed adularia (McConnell, 1965, 1971) and tweed anorthoclase (Smith, McLaren & O'Donnell, 1987; Xu, 1993). There are also out-of-phase domain boundaries in the orthoclase (Fig. 5*b*). Presumably, the out-of-phase boundaries developed during the formation of the modulated structure, similar to boundaries in intermediate plagioclase (McLaren & Marshall, 1974; Miura, 1979). Lattice distortion along the out-of-phase boundaries would be similar to that in a modulated orthoclase proposed by Eggleton & Buseck (1980).

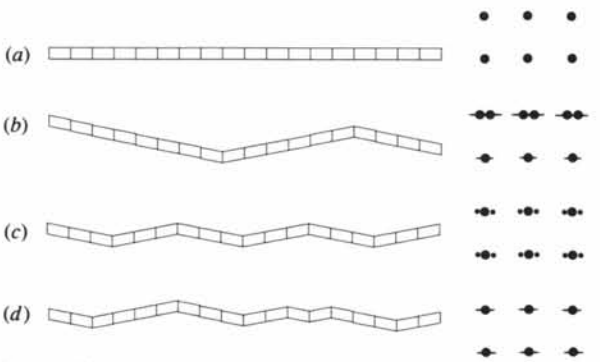

Fig. 3. Different arrangements of triclinic domains in potassium feldspar and their corresponding diffraction patterns. The b^* axis is horizontal. (*a*) Perfectly homogeneous monoclinic crystal. (*b*) Large triclinic domains arranged in a nonperiodic way. (*c*) Fine-scale triclinic domains arranged periodically to form a commensurate modulated structure. (*d*) Fine-scale triclinic domains arranged nonperiodically.

Fig. 6 shows a HRTEM image of a modulated orthoclase sample in the same orientation as that of Fig. 4, showing sinusoidal modulation of the (001) lattice fringes. Every two small blocks in the HRTEM image represent one triclinic subcell along the horizontal direction in Fig. 6 (*i.e.* along the b^* direction). It can be seen in Fig. 6 that there are two kinds of domain with thicknesses of $4b_{sub}$ in twin-related orientations with opposite b_{sub} axes.

Fig. 7 is a schematic structural model for the modulated structure, showing sinusoidal (001) and

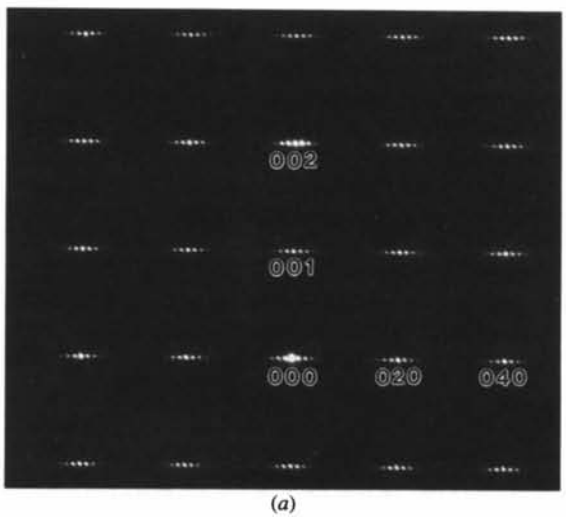

(*a*)

(*b*)

Fig. 4. (*a*) A [100] zone-axis SAED pattern of orthoclase from the Wulian augite monzonite, showing main Bragg reflections and satellite reflections along the b^* direction. (*b*) A bright-field image formed from the transmitted spot (central beam) and its nearby satellite reflections, showing one-dimensional modulation along the *b* axis.

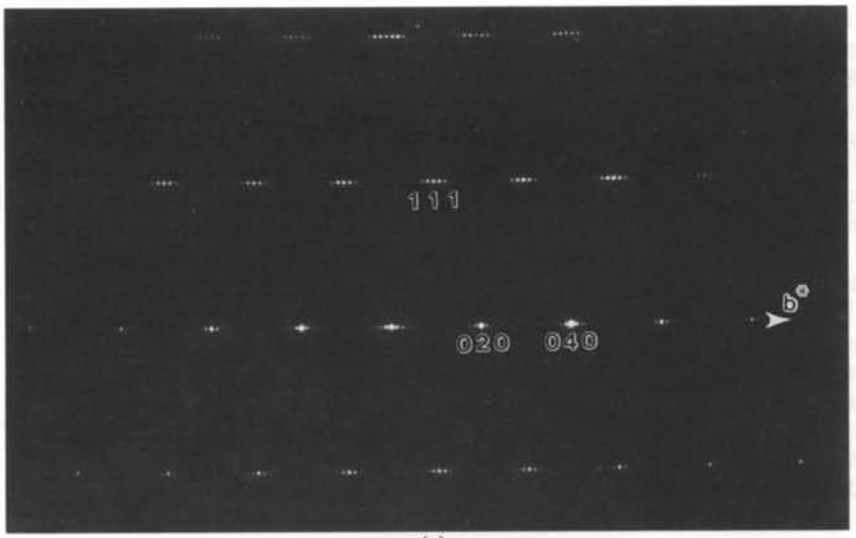

(*a*)

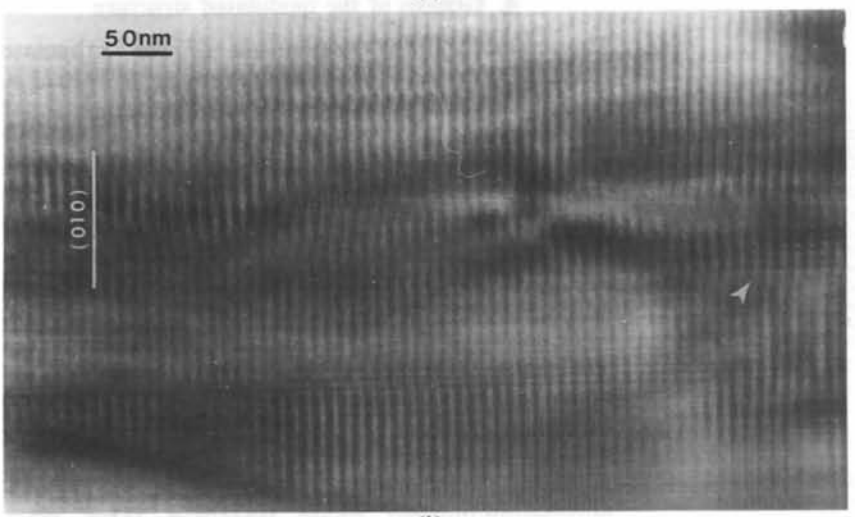

(*b*)

Fig. 5. (*a*) A [10$\bar{1}$] zone-axis SAED pattern showing main Bragg reflections and satellite reflections along the b^* direction. (*b*) Corresponding BF image, showing one-dimensional modulation along the *b* axis, out-of-phase boundaries and an area with weak cross-hatched texture (indicated by an arrow).

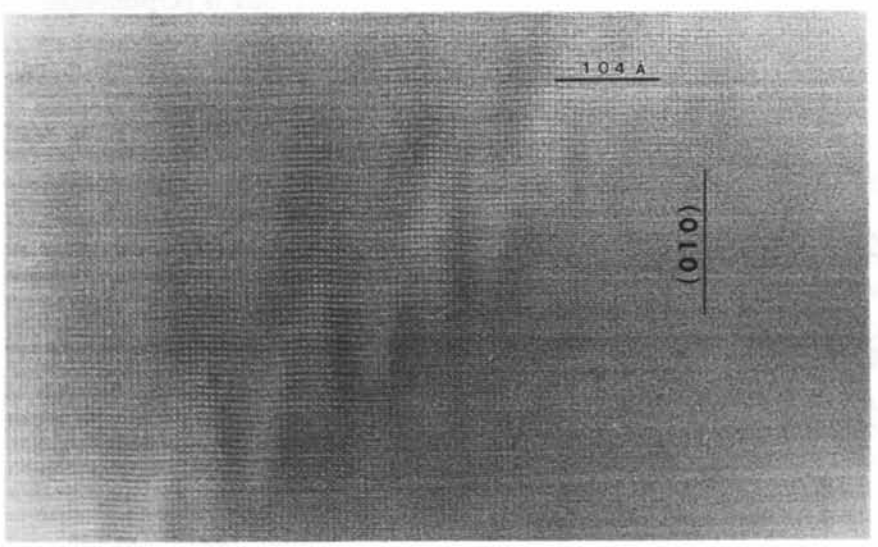

Fig. 6. HRTEM image of Wulian orthoclase with the electron beam parallel to the *a* axis, showing sinusoidal variation of the (001) lattice fringes (*i.e.* modulation waves).

straight (010) lattice planes, which is similar to a model for an orthoclase sample described by Smith (1970) and Eggleton & Buseck (1980). In the model, each block represents one triclinic subcell. An extended supercell is also outlined in Fig. 7. This extended unit cell of modulated orthoclase should be monoclinic with a primitive lattice, rather than a *C*-centered lattice typical of other alkali feldspars. Electron diffraction patterns also show no extinctions for the satellite reflections, which would indicate a primitive unit cell. The relationships between the extended unit-cell parameters (supercell, subscript sup) of the modulated structure and the triclinic subcell (subscript sub) parameters are $a_{sup} \simeq a_{sub}$, $b_{sup} = 8d_{010} \simeq 8b_{sub}$, $c_{sup} \simeq c_{sub}$, $\beta_{sup} \simeq \beta_{sub}$. Given these relationships, the most probable space group for the commensurately modulated orthoclase structure is *Pm*. The mirror planes in the modulated structure can be considered to be mirror-plane positions remaining from the high-temperature monoclinic phase (sanidine). Only one-eighth of the (010) mirror planes in sanidine are preserved in the phase transition to the modulated orthoclase structure.

The structure suggested here for commensurately modulated orthoclase can also be described as the ordered stacking of triclinic (010) layer domains along the *b* axis. In this view, the neighboring triclinic domains are in the albite-twin relationship [*i.e.* they are related by a (010) mirror operation]. Diffraction patterns from orthoclase with this type of modulation will exhibit an average structure with monoclinic symmetry, even though its subcells are distorted in the same fashion as the unit cells of triclinic alkali feldspars.

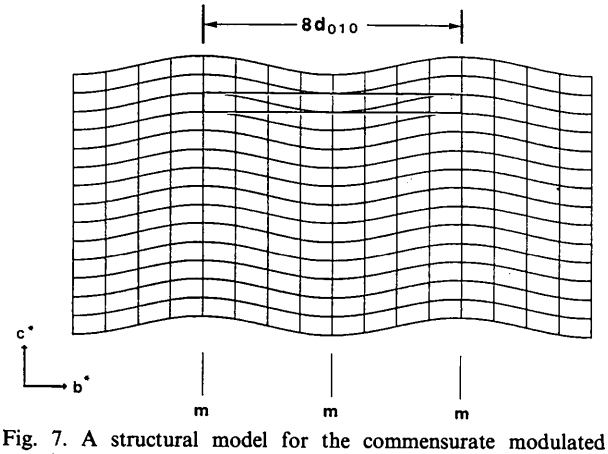

Fig. 7. A structural model for the commensurate modulated orthoclase, showing sinusoidal variation of the (001) lattice planes. Each small block represents a triclinic subcell. Neighboring triclinic domains are in the albite-twin relationship. An extended cell of the modulated structure is also outlined.

4. Genesis of the modulated structure

The crystallization temperature of the orthoclase from Wulian has been estimated as 973–1023 K (Pan, 1986). It is well known that potassium feldspar crystallized in that temperature range will display monoclinic symmetry (*i.e.* it is sanidine) with a relatively disordered Al–Si distribution (Smith, 1974; Ribbe, 1983) (see Fig. 1). Ordering of Al–Si in the tetrahedral sites can take place as the feldspar cools, for a slow enough cooling rate. According to published phase diagrams for alkali feldspars (Smith, 1974; Smith & Brown, 1988; Yund, 1983), potassium feldspar with composition Or_{85} will encounter the phase-transition boundary from monoclinic ($C2/m$) sanidine to triclinic ($C\bar{1}$) microcline at a considerably higher temperature than that at which coherent exsolution involving K–Na occurs (Fig. 1). The Al–Si-ordering-induced phase transition takes place before K–Na exsolution occurs. In addition, the orientation of the superstructure is perpendicular to

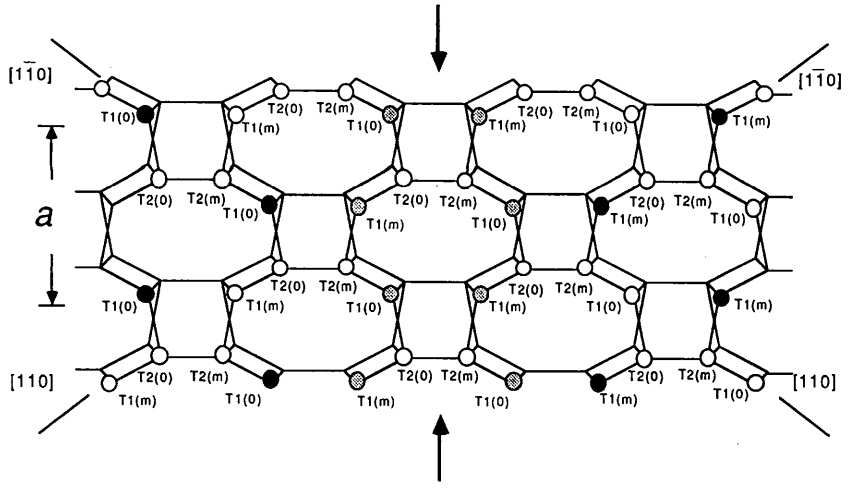

Fig. 8. An idealized projection of modulated orthoclase down the c^* direction onto the *ab* plane, showing possible distribution of Al atoms in the T_1 sites near a domain boundary (indicated by arrows). The boundary between neighboring domains can be interpreted as an albite-twin boundary between microcline blocks but it is also a true mirror plane of the commensurate modulated structure taken as a whole. It is likely that the Al–Si distribution near the boundary is relatively disordered, at least between the $T_{1(m)}$ and $T_{1(0)}$ sites. Unfilled circles represent silicon-dominant $T_{2(m)}$ and $T_{2(0)}$ sites; fully filled circles represent aluminium-dominant $T_{1(m)}$ and $T_{1(0)}$ sites.

those reported for exsolution in alkali feldspars. Given the phase diagram and the modulation orientation, it seems very unlikely that the formation of the observed modulation involves K–Na unmixing. It is far more likely that it arises due to Si–Al ordering. The sanidine–microcline phase transition is characterized by preferential ordering of Al atoms into one of the T_1 sites (*i.e.* either $T_{1(0)}$ or $T_{1(m)}$ sites – see above) from T_2 sites in each domain, which are symmetrically related by the mirror and twofold symmetry of sanidine. Preservation of some of the monoclinic point-group symmetry elements as twinning operations leads to the formation of albite and pericline twins below the phase-transition temperature (Ribbe, 1983).

When the aluminium occupancies in the $T_{1(0)}$ and $T_{1(m)}$ sites become unequal, a domain can be considered to have triclinic symmetry. If the twin domains forming between the triclinic domains are arranged periodically, a superstructure forms (Ribbe, 1983). A view of the probable Al–Si distribution near the domain boundaries of the modulated orthoclase is schematically illustrated in Fig. 8, which shows the albite twin-related ordering patterns in the domains to the left and right of the boundary. We hypothesize that the Al–Si distribution in and near the boundary positions is relatively disordered in the $T_{1(m)}$ and $T_{1(0)}$ sites with respect to other areas. There should be nearly equal aluminium occupancies in the $T_{2(m)}$ and $T_{2(0)}$ sites of triclinic domains (Ribbe, 1983), even though the diagram does not show them. Thus, not only the mirror symmetry but also the Si–Al ordering pattern of the high-temperature monoclinic structure may be preserved at the domain boundaries of the modulated orthoclase structure.

The curved or sinusoidal modulation of (001) lattice fringes implies a sinusoidal variation in the deviation of the unit-cell shapes from monoclinic symmetry, sometimes called 'triclinicity' or Δ. Therefore, the modulated orthoclase structure could also be described as an alternation of relatively ordered and relatively disordered (010) slabs along the b axis. Periodic arrangement of triclinic domains is related to the kinetics of Al–Si ordering in potassium feldspar and, in some ways, it is similar to the early-stage ordering in cubic lattice metals described by Cook, de Fontaine & Hilliard (1969), even though the feldspar structure is more complex. The ordered crystal with domain structure may be modulated by a modulation wave under certain conditions during the early-stage ordering (Cook *et al.*, 1969).

5. Concluding remarks

Orthoclase in an augite monzonite from Shandong shows an ordered commensurate modulated structure with a supercell having $b_{sup} = 8b_{sub}$. On the basis of electron diffraction, TEM imaging experiments and the alkali feldspar phase diagram, the modulated structure appears to consist of periodic triclinic (010) layer domains in the albite-twin relationship. HRTEM images directly show that the subcells of the structure periodically deviate in position and shape from those of the monoclinic lattice of sanidine. The modulated structure could also be considered as a periodic alternation of slabs having relatively good Si–Al order with relatively disordered slabs along the b axis.

The modulated structure probably forms as a metastable intermediate structure by ordering of Al atoms into $T_{1(0)}$ and $T_{1(m)}$ sites in different domains at the arrested phase transition from sanidine ($C2/m$) to microcline ($C\bar{1}$). It is a commensurate structure that can be described most simply as unit-cell-scale twinning of the microcline structure.

This work was supported by the NNSF of China, the NSF of the USA (grant EAR89-03630) and Nanjing University. Electron microscopy was carried out in the Laboratory of Solid State Microstructure, Nanjing University, and in the HRTEM/AEM laboratory at Johns Hopkins University. We thank John Ferry for his helpful comments.

References

COOK, H. E., DE FONTAINE, D. & HILLIARD, J. E. (1969). *Acta Metall.* **17**, 765–773.

EGGLETON, R. A. & BUSECK, P. R. (1980). *Contrib. Mineral. Petrol.* **74**, 123–133.

GOLDSMITH, J. R. & LAVES, F. (1954). *Geochim. Cosmochim. Acta*, **6**, 100–118.

LAVES, F. (1950). *J. Geol.* **58**, 548–571.

MCCONNELL, J. D. C. (1965). *Philos. Mag.* **11**, 1289–1301.

MCCONNELL, J. D. C. (1971). *Mineral. Mag.* **38**, 1–20.

MCLAREN, A. C. (1984). *Feldspars and Feldspathoids*, edited by W. L. BROWN, pp. 373–404. Dordrecht: Reidel.

MCLAREN, A. C. & FITZ GERALD, J. D. (1988). *Phys. Chem. Mineral.* **14**, 261–292.

MCLAREN, A. C. & MACKENZIE, W. S. (1976). *Phys. Status Solidi A*, **33**, 491–495.

MCLAREN, A. C. & MARSHALL, D. B. (1974). *Contrib. Mineral. Petrol.* **44**, 237–249.

MARFUNIN, A. S. (1966). *The Feldspars: Phase Relations, Optical Properties, and Geological Distribution.* Jerusalem: Israel Prog. Sci. Translations.

MIURA, Y. (1979). *Modulated Structures – 1979, AIP Conference Proceedings* No. 53, edited by J. M. COWLEY, J. B. COHEN & B. J. WUENSCH, pp. 314–316. New York: American Institute of Physics.

NISSEN, H.-U. (1967). *Contrib. Mineral. Petrol.* **16**, 354–360.

PAN, Y. (1986). Thesis, Department of Earth Sciences, Nanjing Univ., Nanjing, People's Republic of China.

PARSONS, I. (1984). *Feldspars and Feldspathoids*, edited by W. L. BROWN, pp. 317–371. Dordrecht: Reidel.

RIBBE, P. H. (1983). Editor. *Feldspar Mineralogy, Reviews in Mineralogy*, Vol. 2, pp. 21–55. Washington, DC: Mineralogical Society of America.

SMITH, J. V. (1970). *Lithos*, **3**, 145–160.
SMITH, J. V. (1974). *Feldspar Minerals*, Vol. 1, pp. 33–54, 208–228. Heidelberg: Springer-Verlag.
SMITH, J. V. & BROWN, W. L. (1988). *Feldspar Minerals*, Vol. 1, pp. 50–84, 127–129, 224–248, 416–436, 461–477. Heidelberg: Springer-Verlag.
SMITH, K. L., MCLAREN, A. C. & O'DONNELL, R. G. (1987). *Can. J. Earth Sci.* **24**, 528–543.
SU, S. C., BLOSS, F. D., RIBBE, P. H. & STEWART, D. B. (1984). *Am. Mineral.* **69**, 440–448.
WRIGHT, T. L. & STEWART, D. B. (1968). *Am. Mineral.* **53**, 38–87.
XU, H. (1993). PhD dissertation, Johns Hopkins Univ., Baltimore, USA.
YUND, R. A. (1983). *Feldspar Mineralogy, Reviews in Mineralogy*, Vol. 2, edited by P. H. RIBBE, pp. 177–202. Washington, DC: Mineralogical Society of America.

Acta Cryst. (1995). A**51**, 60–69

The Vertex Contribution to the Kirste–Porod Term

BY SALVINO CICCARIELLO

Dipartimento di Fisica 'G. Galilei' and Sezione INFM, via Marzolo 8, *I*-35131 *Padova, Italy*

AND ROGER SOBRY

Laboratory of Experimental Physics, Institut of Physics B5, University of Liège, Sart Tilman, B-4000 *Liège, Belgium*

(*Received* 7 *February* 1994; *accepted* 28 *June* 1994)

Abstract

It is shown that, close to the origin, the correlation function $[\gamma(r)]$ of any N-component sample with interfaces made up of planar facets is always a third-degree polynomial in r. Hence, the only monotonically decreasing terms present in the asymptotic expansion of the relevant small-angle scattered intensity are the Porod $[-2\gamma'(0^+)/h^4]$ and the Kirste–Porod $[4\gamma^{(3)}(0^+)/h^6]$ contributions. The latter contribution is non-zero owing to the contributions arising from each vertex of the interphase surfaces. The general vertex contribution is evaluated in closed form and the $\gamma^{(3)}(0^+)$ values relevant to the regular polyhedra are reported.

I. Introduction

In the theory of small-angle scattering (SAS), samples are generally modelled as consisting of N homogeneous phases, each characterized by a constant electron or scattering-length-density value n_i and by the occupied sample subregion $\mathbf{V}_i$, $i = 1, ..., N$. The standard normalized scattered intensity $I(\mathbf{h})$ (Porod, 1982) is the Fourier transform of $\gamma(\mathbf{r})$, the so-called sample correlation function (CF). For isotropic samples, these quantities depend, respectively, only on h and r and are related by

$$I(h) = (4\pi \mathbf{V}\langle\eta^2\rangle/h)\int_0^\infty r\gamma(r)\sin(hr)\mathrm{d}r, \qquad (1.1)$$

where*

$$\gamma(r) = 1 - \sum_{1\le i<j\le N}[(n_i - n_j)^2/\langle\eta^2\rangle]P_{ij}(r), \qquad (1.2)$$

$$P_{ij}(r) \equiv (1/4\pi\mathbf{V})\int \mathrm{d}\hat{\omega}\int_{R^3}\mathrm{d}v'\rho_i(\mathbf{r}')\rho_j(\mathbf{r}' + r\hat{\omega}), \qquad (1.3)$$

$$\langle\eta^2\rangle = \sum_{1\le i\le N}(n_i - \langle n\rangle)^2\phi_i = \sum_{1\le i<j\le N}(n_i - n_j)^2\phi_i\phi_j. \qquad (1.4)$$

It should be noted that (1.2) and (1.3) do not require that interfaces are convex and that the sample is dilute. However, when the conditions are fulfilled, the second derivative of $\gamma(r)$, denoted $\gamma^{(2)}(r)$ or $\gamma''(r)$, coincides with Porod's intersect distribution function. According to a general theorem on Fourier transforms (Erdélyi, 1956), the behaviour of $I(h)$ at large h is related to the behaviour of the $\gamma(r)$ derivatives $[\gamma^{(n)}(r),\ n = 1, 2, ...]$ around the origin and around those r values, denoted δ_l $(l = 1, ..., M)$,

* The meanings of the symbols involved in these equations are as follows: $h \equiv (4\pi/\lambda)\sin(\theta/2)$ with θ and λ respectively denoting the scattering angle and the beam-particle wavelength; $\mathbf{V}$ is the sample volume; $\phi_i \equiv \mathbf{V}_i/\mathbf{V}$ is the volume fraction of the ith phase; $\rho_i(\mathbf{r})$ is defined as being equal to unity when the tip of the position vector $\mathbf{r}$ falls inside region $\mathbf{V}_i$ and equal to zero elsewhere, and $\hat{\omega}$ is a unit vector that can assume all possible orientations. The bold capital symbols $\mathbf{V}$ and $\mathbf{V}_i$ should not be confused with vectors, which are always denoted by bold small capitals or, when they are unit vectors, by greek letters with carets.